

Electronic Support Information (ESI)

In situ hydrogelation of bicalutamide-peptide conjugates at prostate tissue for smart drug release based on pH and enzymatic activity

Suyun He,^a Leixia Mei,^a Can Wu,^a Mingtao Tao,^a Ziran Zhai,^a Keming Xu^{*a,b} and Wenyong Zhong^{*a,b}

^a Department of Chemistry, China Pharmaceutical University, Nanjing 210009, P. R. China.

^b Key Laboratory of Biomedical Functional Materials, China Pharmaceutical University, Nanjing 210009, P. R. China.

E-mail: wyzhong@cpu.edu.cn

Table of contents

Experimental

Fig. S1. The chemical structures and optical images of screening entries

Fig. S2. Syntheses route of **ID-1-BLT**

Fig. S3. Mass spectrum of **Nap-1**

Fig. S4. HPLC spectrum of **Nap-1**

Fig. S5. Mass spectra of **ID-1**

Fig. S6. HPLC spectrum of **ID-1**

Fig. S7. ¹HNMR (300 MHz, DMSO) spectrum of **ID-1**

Fig. S8. Mass spectrum BLT-SA

Fig. S9. HPLC spectrum of BLT-SA

Fig. S10. ¹HNMR (300 MHz, DMSO) spectrum of BLT-SA

Fig. S11. HPLC spectrum of **ID-1-BLT**

Fig. S12. Mass spectrum of **ID-1-BLT**

Fig. S13. ¹HNMR spectrum (300 MHz, DMSO) of **ID-1-BLT**

Fig. S14. FT-IR spectra of **ID-1** and **ID-1-BLT**

Fig. S15. FT-IR spectra of **ID-1-BLT** powder and lyophilized gel

Fig. S16. Dynamic frequency sweep of **ID-1-BLT**

Fig. S17. Dynamic time sweep of **ID-1-BLT**

Fig. S18. Standard curve of BLT

Fig. S19. Standard curve of **ID-1-BLT**

Fig. S20. Degradation ratio of **ID-1-BLT** incubated with different CES activity for 72h

Fig. S21. Cell viability of DU145 after 24 h and 48 h treatment of **ID-1**

Fig. S22. CES activity of DU145 and NIH3T3 cells with Calcein-AM

Fig. S23. H&E staining of the prostate tissue after intra-gland injections of **ID-1** peptide and saline in rats for 7 days

Table. S1. The parameters fitted with Ritger-Peppas models for 72 h drug release of **ID-1-BLT** in release buffers of varying pH

Table. S2. The parameters fitted with Ritger-Peppas models for 72 h drug release of **ID-1-BLT** in release buffers with varying units of CES

Experimental

S1 Drug release study of ID-1-BLT hydrogels *in vitro*

S1.1 Standard curves of BLT and ID-1-BLT by HPLC

2.50 mg BLT or 9.40 mg **ID-1-BLT** was precisely weighed and dissolved with diluent (acetonitrile: water = 2:1, v/v) to 25 mL as stock solution (0.100 mg/mL or 0.375 mg/mL), respectively. 0.2 mL, 0.4 mL, 0.8 mL, 1.6 mL, 3.2 mL, 6.4 mL of stock solutions were precisely measured and volumed to 10 mL as working solutions, respectively. All of the working solutions were measure by HPLC under the same condition which was carried out on a SHIMADZU HPLC system, eluting with 20% CH₃CN (0.1% of TFA) to 80% CH₃CN (0.1% of TFA) in water (0.1% of TFA) on a SEPAX GP-C18 column (4.6×250 mm) with 5 μm pore size and 120 Å particle size. The peak area-concentration (A-C) linear relation equation of BLT was $A=33753*C-25845$, $R^2=0.9982$, and that of **ID-1-BLT** was $A=2231.9*C-1150.2$, $R^2=0.9997$.

S1.2 Degradation ratio of ID-1-BLT incubated with varying CES activity

ID-1-BLT stock solution (2.0 wt%) was prepared and filtered by 0.22 μm filter. 200 μL of stock solution was diluted 10 times with 10 mM borate buffer (pH 8.0) to 2 mg/ mL. Corresponding amount of CES was added to prepare 10, 30, 50 U/mL CES-**ID-1-BLT** test solution. After stirring under 37 °C, 500 μL of mixture was taken out at fixed time points (1 h, 3 h, 7 h, 12 h, 24 h, 48 h, 72 h) and 2-fold volume acetonitrile was added to inactivate CES. The mixture was filtered by 0.22 μm filter, then concentrations of **ID-1-BLT** and BLT were quantified by HPLC with standard curves of **ID-1-BLT** and BLT. Triplicates experiments were done.

S1.3 Release mechanism

To provide an explanation about the conceivable mechanism of the drug release behavior of **ID-1-BLT** hydrogels, the data were analyzed fitting to the following empirical equations:

Model: Ritger-Peppas equation

$$M_t / M_\infty = k \cdot t^n$$

Where M_t / M_∞ is fractional drug release, M_t is the amount of drug released at time t , M_∞ is the maximum amount of drug released at time ∞ , t is the release time, k is a rate constant of kinetic release, and n is the diffusion exponent, characteristic of the drug release mechanism. For $n < 0.45$, it indicates that the release behavior follows the Fickian diffusion, whereas the non-Fickian release behavior has a value of n between 0.45 and 1.00 since our hydrogels belong to non-swelling cylindrical devices.

S2 CES activity of DU145 and NIH3T3 cells with Calcein-AM

5 uL of Calcein-AM fluorescent dye stock solution (1 mg/mL) was taken and added to 2.5 mL of DMEM-high glucose and RPMI-1640 cell culture media respectively. The Calcein-AM fluorescent dye solution (2 ug/mL) were obtained.

500 μL NIH3T3 or DU145 cell suspensions with the cell density of 8×10^4 cells per well were inoculated in each well of 24-well culture plate. After incubation for 24 h at 37 °C, supernatant

were aspirated. Each well of 24-well culture plate was washed twice by PBS solution and 400 μL of Calcein-AM fluorescent dye solution were added into 24-well culture plate. After incubation under 37°C for 1 h, supernatant were aspirated and each well of 24-well culture plate was washed twice by PBS solution. 500 μL of PBS was added into 24-well culture plate and observed under fluorescence microscope (Olympus IX71, Japan). Three experiments were done.

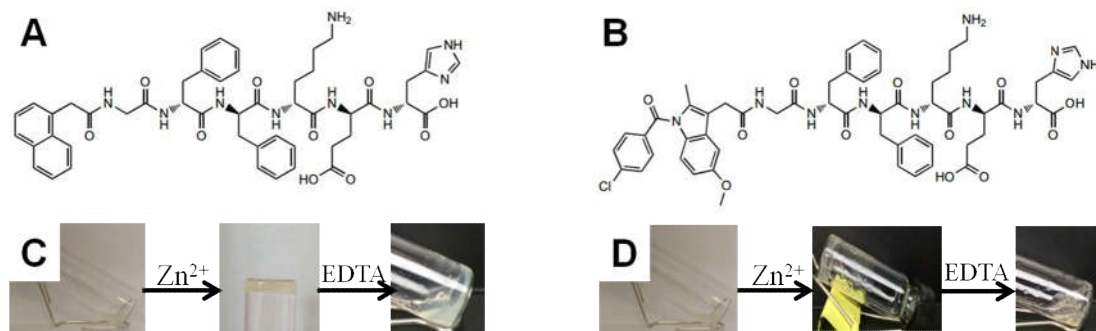


Fig. S1. The chemical structures and optical images of screening entries. (A) The chemical structure of **Nap-1**; (B) The chemical structure of **ID-1**; (C) Optical images of sol-gel transitions of **Nap-1** with Zn^{2+} and EDTA. (D) Optical images of sol-gel transitions of **ID-1** with Zn^{2+} and EDTA.

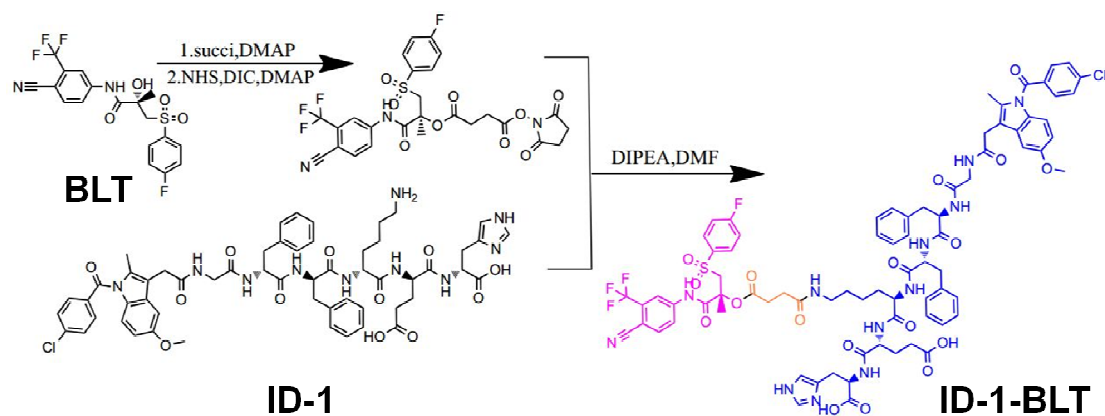


Fig. S2. Syntheses route of **ID-1-BLT**

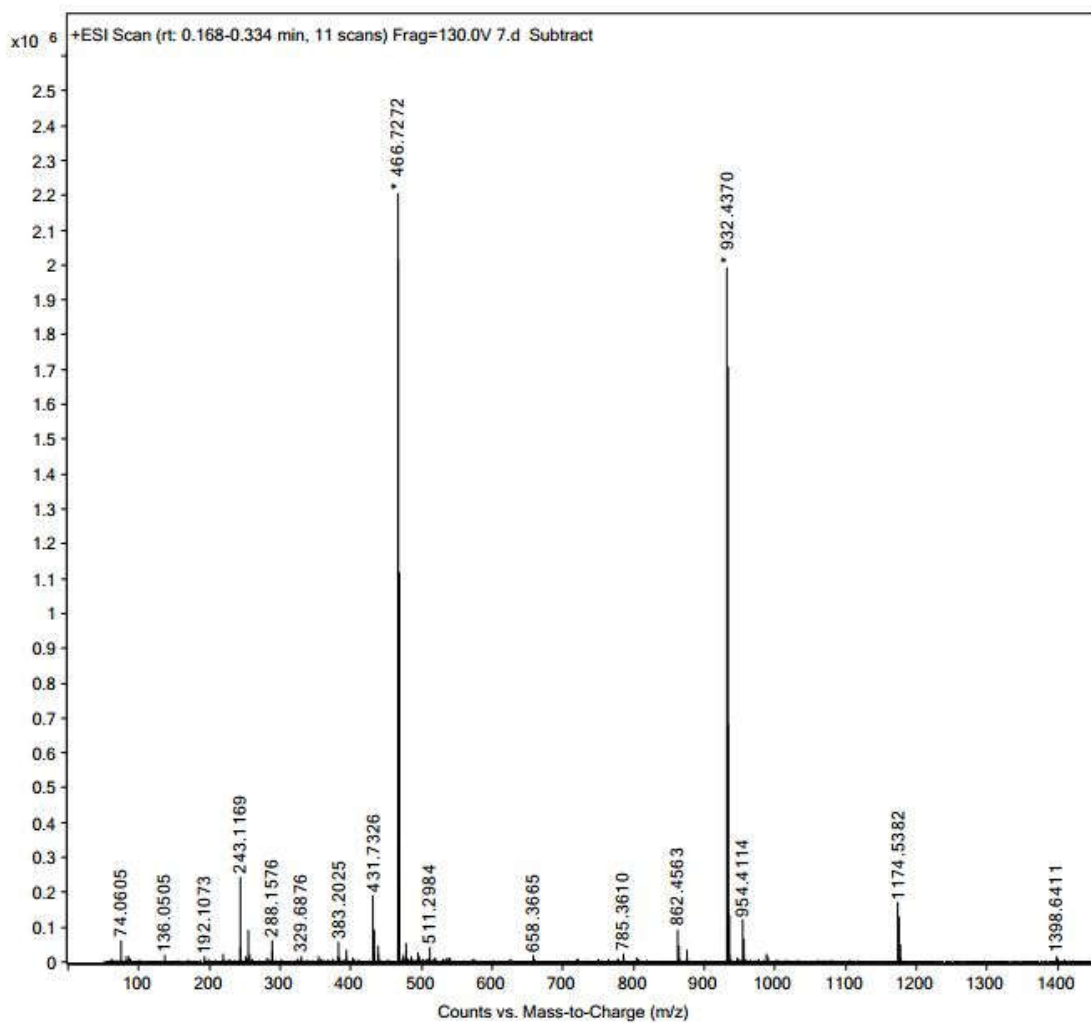


Fig. S3. Mass spectrum of **Nap-1**: C₄₉H₅₇N₉O₁₀, calc. MW=932.03, obsvd. ESI+MS: M⁺=932.4370, [M+H]⁺/2=466.7272.

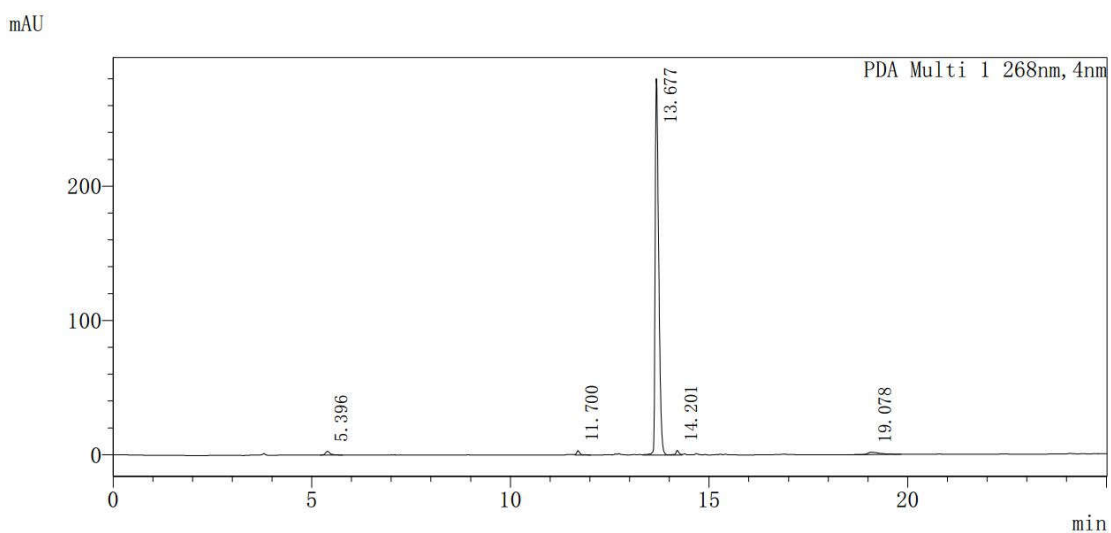


Fig. S4. HPLC spectrum of **Nap-1**

Under high performance liquid chromatographic (HPLC) condition which was carried out on a SHIMADZU HPLC system, eluting with 20% CH₃CN (0.1% of TFA) to 80% CH₃CN (0.1% of

TFA) in water (0.1% of TFA) on a SEPAX GP-C18 column (4.6×250 mm) with 5 μm pore size and 120 Å particle size, the t_R of **Nap-1** were 13.677 min and the purity were 94.5%.

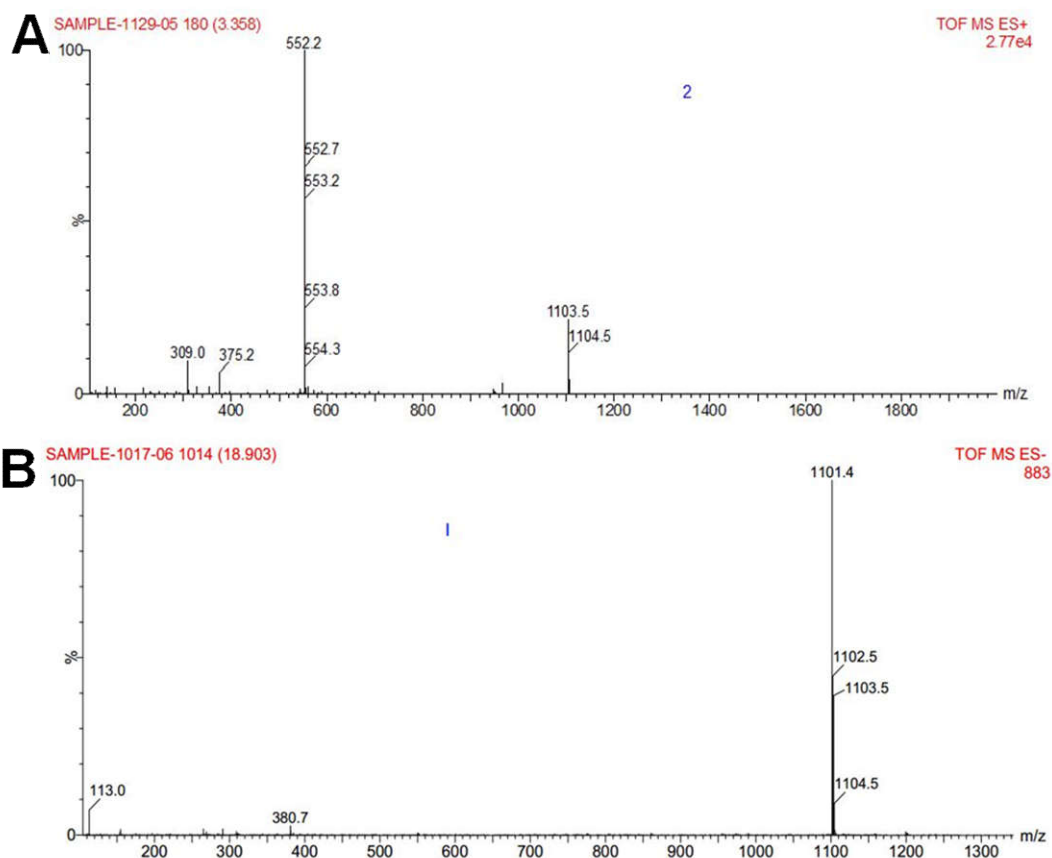


Fig. S5. Mass spectra of **ID-1**: $C_{56}H_{63}ClN_{10}O_{12}$, calc. MW=1103.6, obsvd. (A) ESI+MS: M^+ =1103.5, $[M+H]^+$ =1104.5, $[M+H]^+/2$ =552.2; (B) ESI-MS: $[M-2H]^-$ =1101.4, $[M-H]^-$ =1102.5.

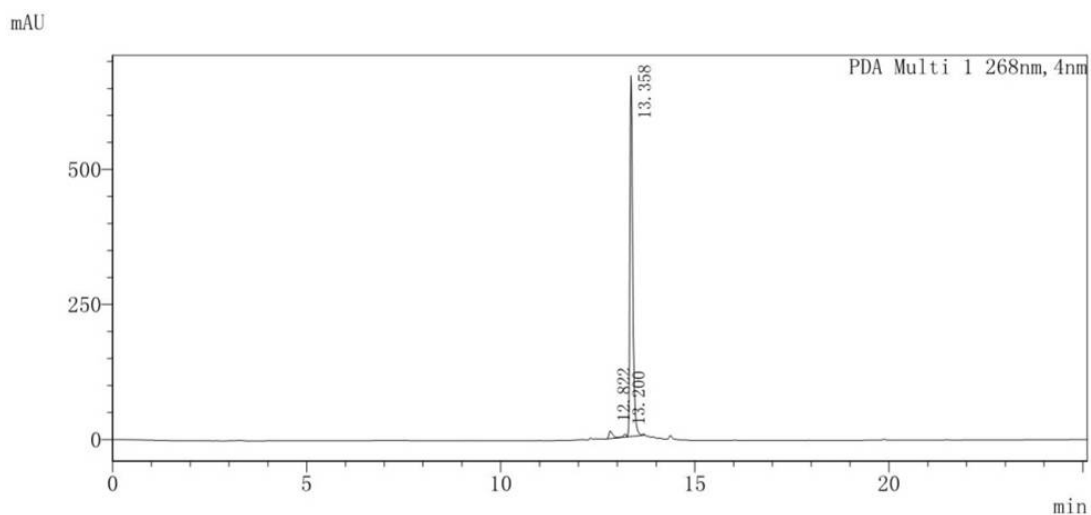


Fig. S6. HPLC spectrum of **ID-1**

Under the same HPLC condition, the t_R of **ID-1** were 13.358 min and the purity were 96.3%.

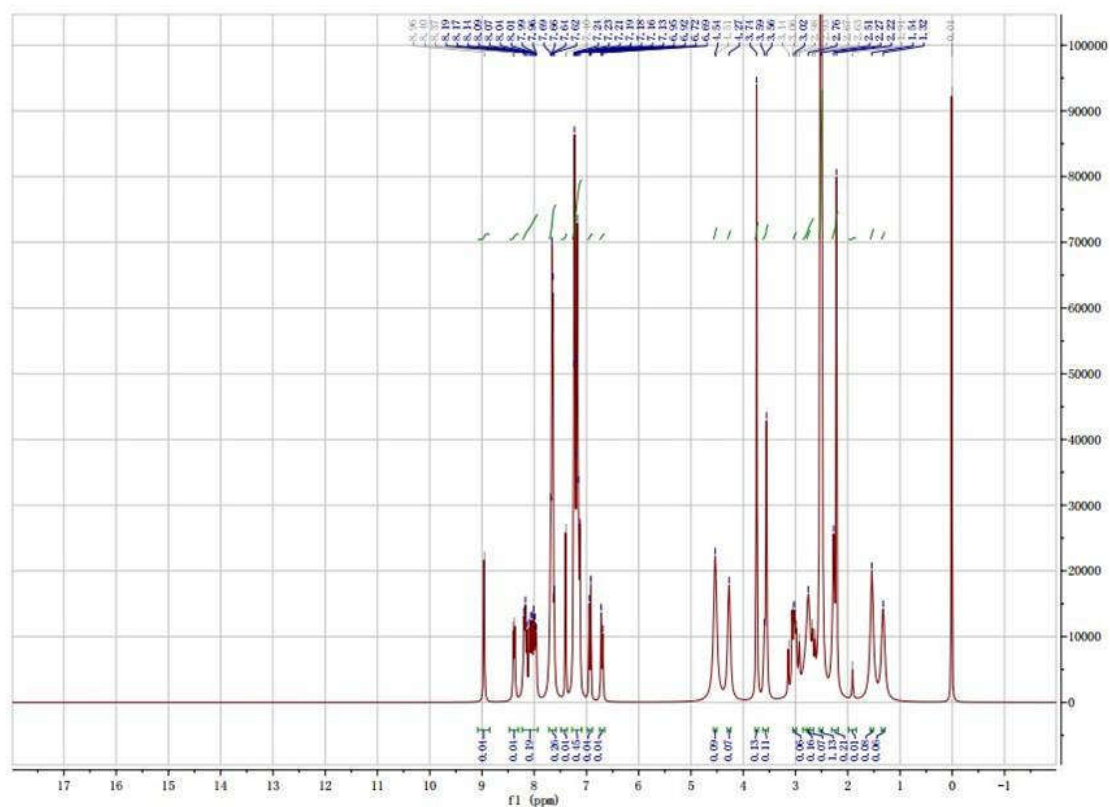


Fig. S7. ^1H NMR (300 MHz, DMSO) spectrum of **ID-1**:

δ 8.96 (s, H), 8.40~8.37 (d, H), 8.19~7.96 (m, 6H), 7.69~7.62 (m, 8H), 7.40 (s, H), 7.24~7.13 (m, 13H), 6.95~6.92 (d, H), 6.72~6.69 (d, H), 4.54~4.27 (m, 5H), 3.74~3.56 (d, 7H), 3.14~2.93 (m, 2H), 2.75~2.63 (m, 7H), 2.27~2.22 (d, 6H), 1.54~1.32 (d, 4H).

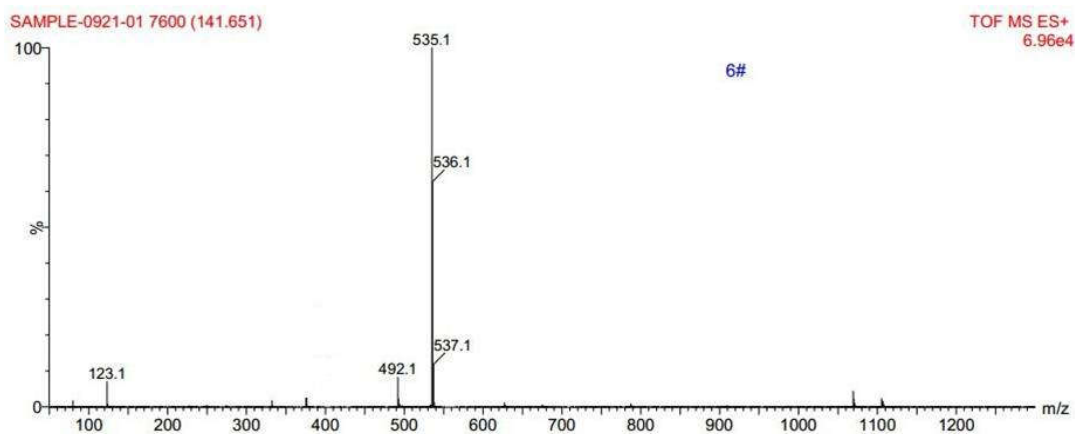


Fig. S8. Mass spectrum BLT-SA: $\text{C}_{24}\text{H}_{20}\text{N}_2\text{O}_8$, ESI-MS: calc.MW=535.4, obsvd. ESI+MS: $[\text{M}+\text{H}]^+=535.1$.

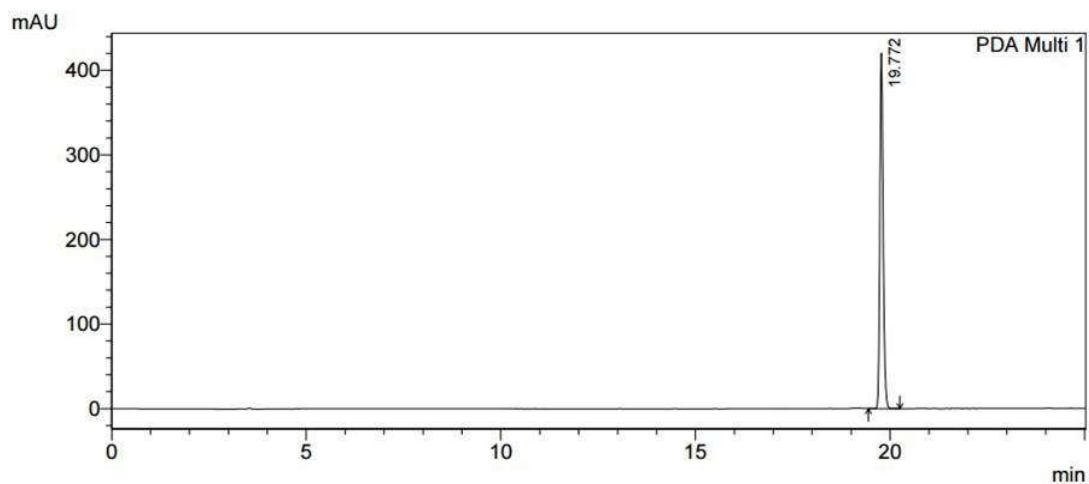


Fig. S9. HPLC spectrum of BLT-SA

Under the same HPLC condition, the t_R of BLT-SA were 19.772 min and the purity were 99.5%.

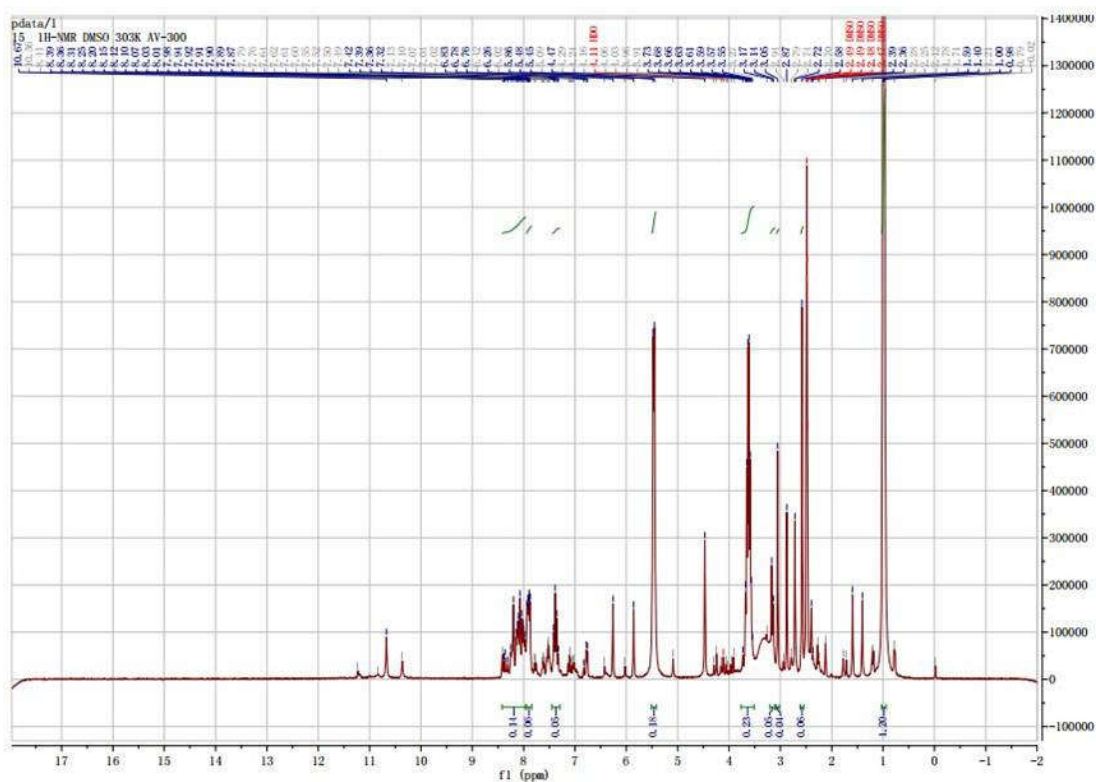


Fig. S10. $^1\text{H-NMR}$ (300 MHz, DMSO) spectrum of **BLT-SA**:

δ 8.39~8.03 (m, H), 7.94~7.87 (m, H), 7.42~7.32 (q, H), 5.45(s, 2H), 3.73~3.55 (m, 2H), 3.17~3.05 (t, H), 2.58 (s, H), 1.00~0.98 (d, 10H).

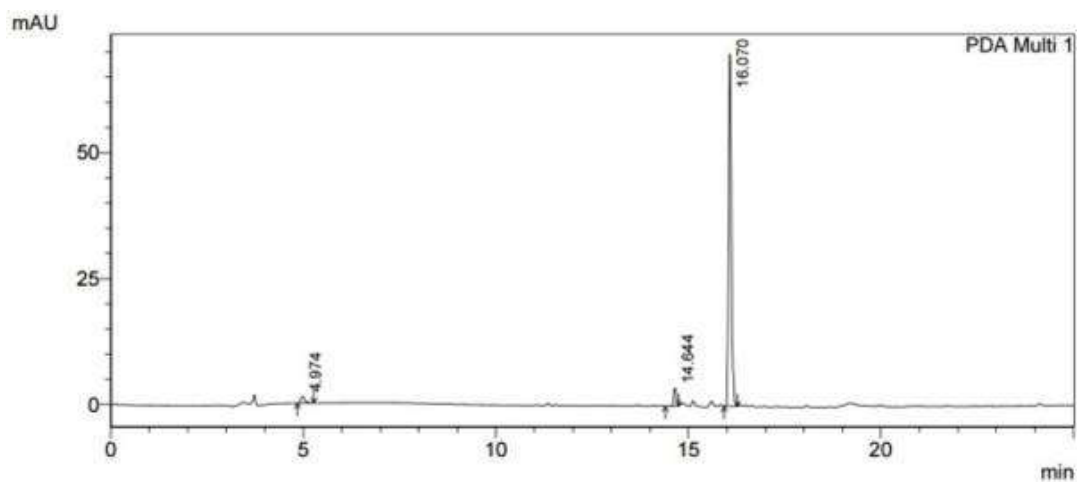


Fig. S11. HPLC spectrum of **ID-1-BLT**

Under the same HPLC condition, the t_R of **ID-1-BLT** were 16.070 min and the purity were 94.5%.

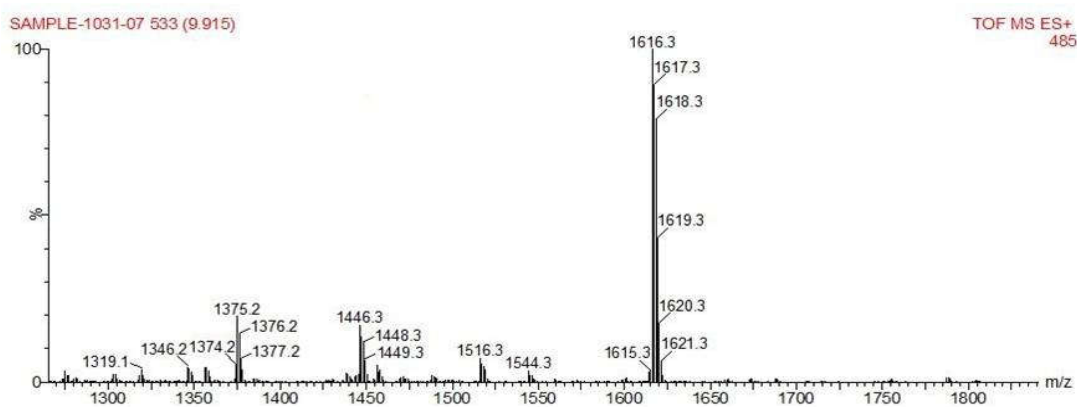
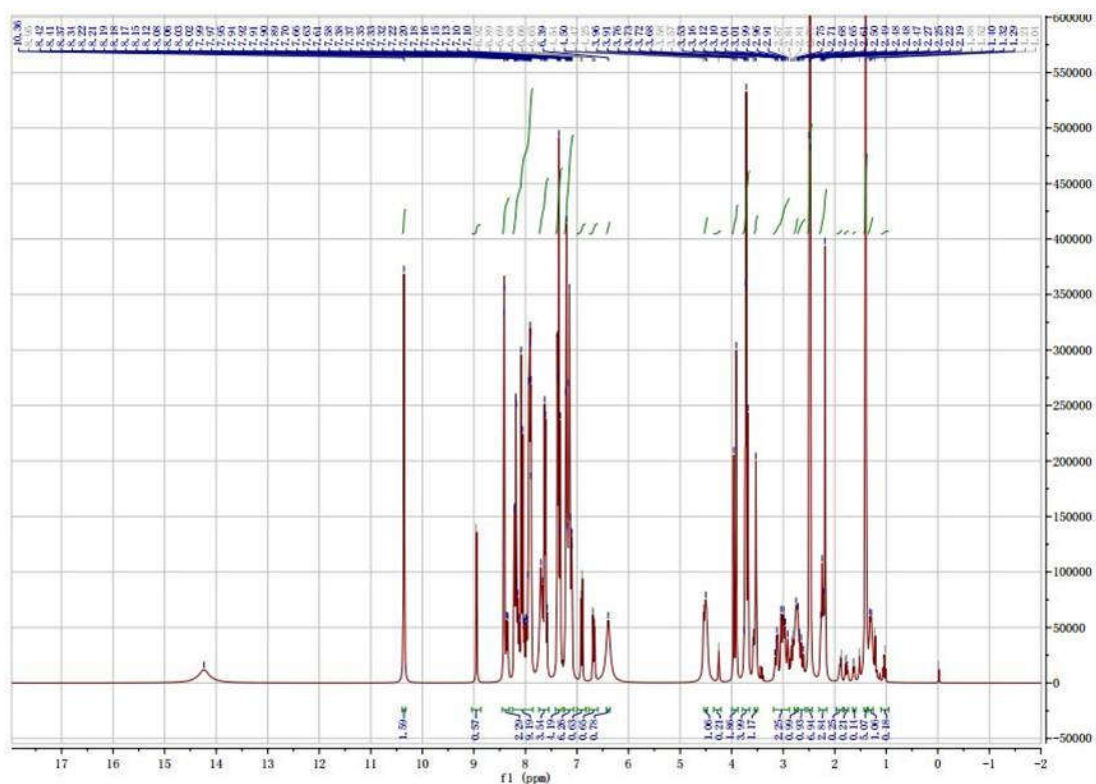


Fig. S12. Mass spectrum of **ID-1-BLT**: $C_{78}H_{79}ClF_4N_{12}O_{18}S$, calc.MW=1616.0, obsvd. ESI+MS: M^+ =1616.3, $[M+H]^+$ =1617.3, $[M+2H]^+$ =1618.3.



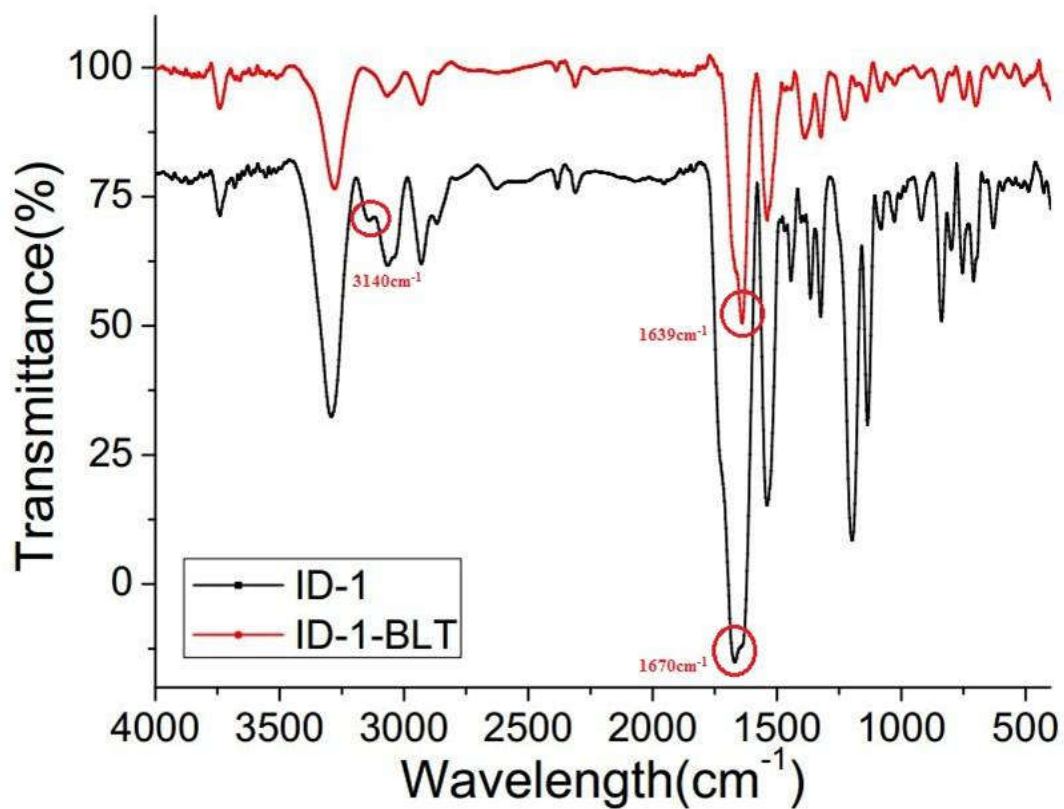


Fig. S14. FT-IR spectra of ID-1 and ID-1-BLT

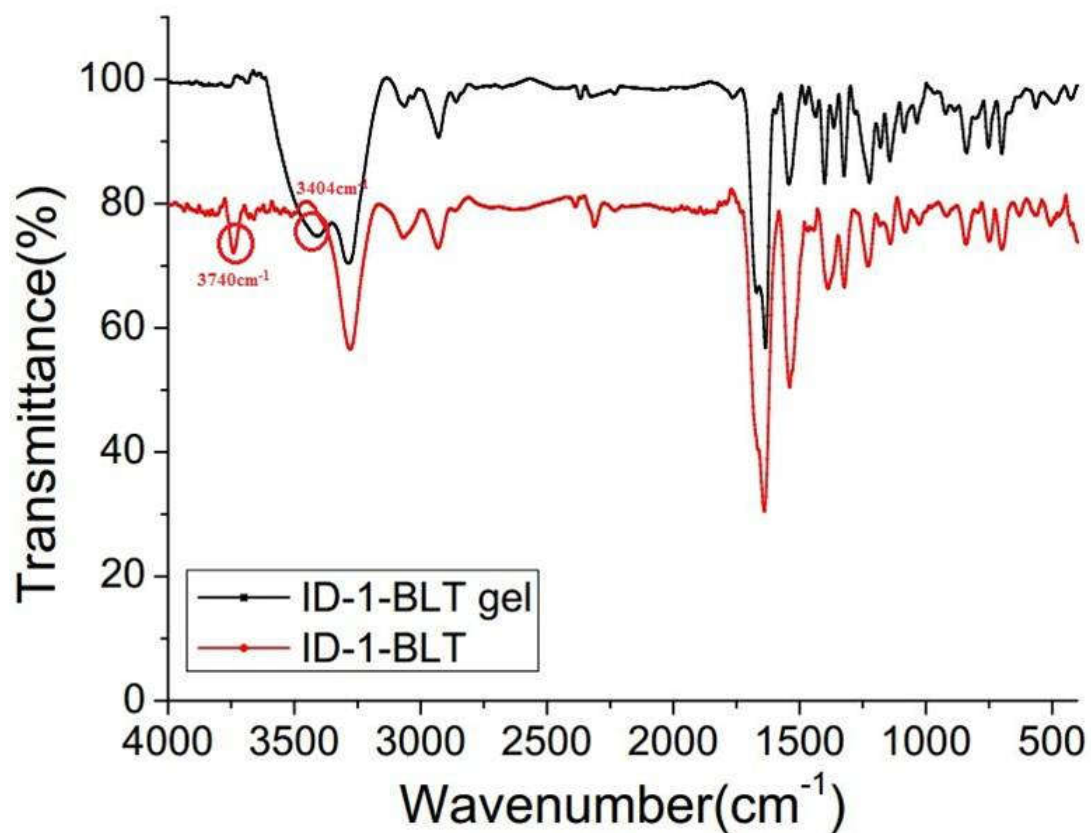


Fig. S15. FT-IR spectra of ID-1-BLT powder and lyophilized gel

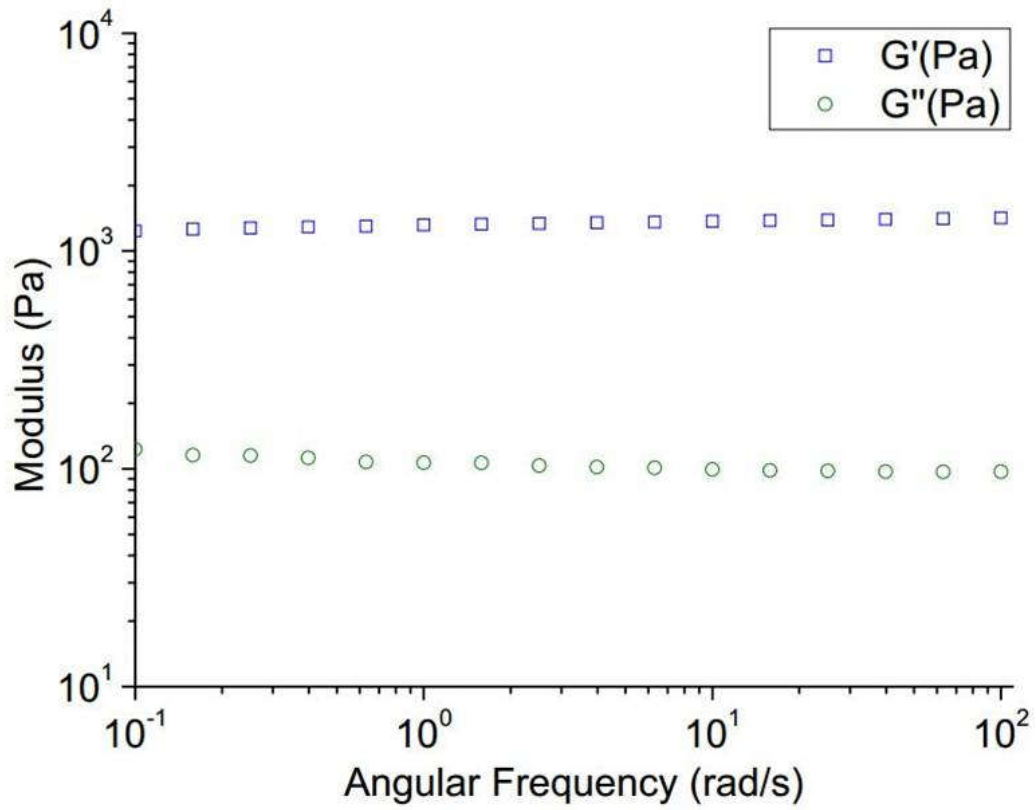


Fig. S16. Dynamic frequency sweep of ID-1-BLT

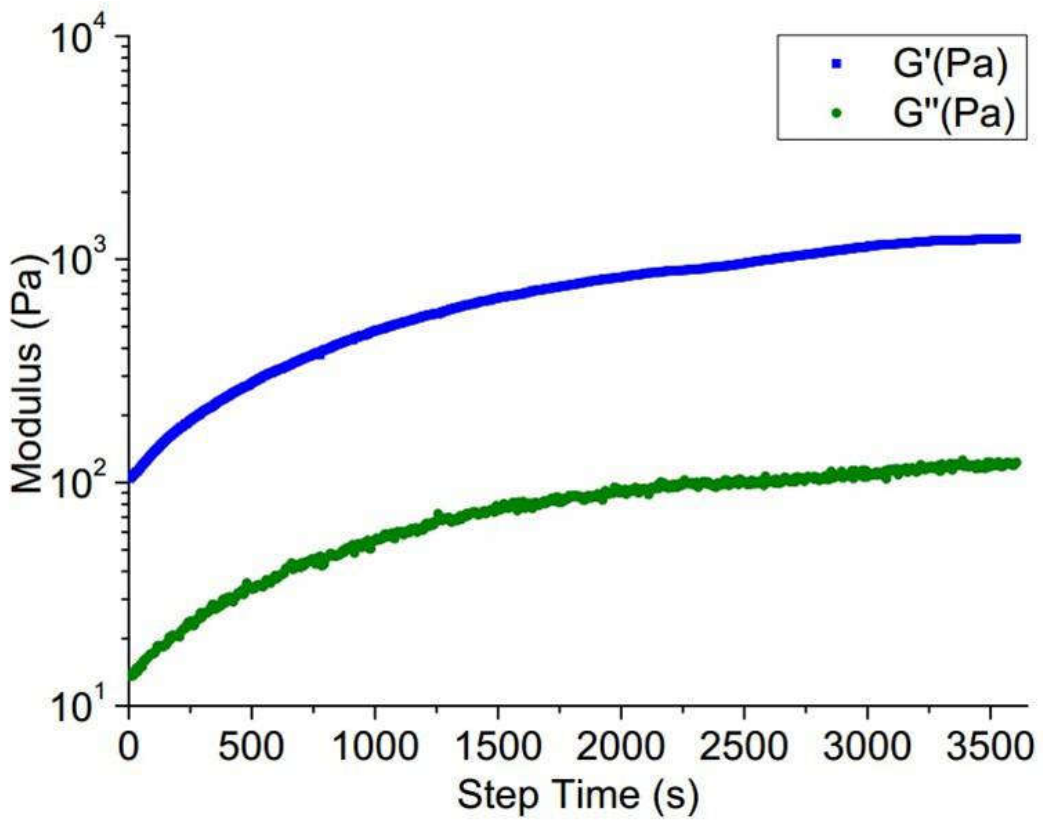


Fig. S17. Dynamic time sweep of ID-1-BLT

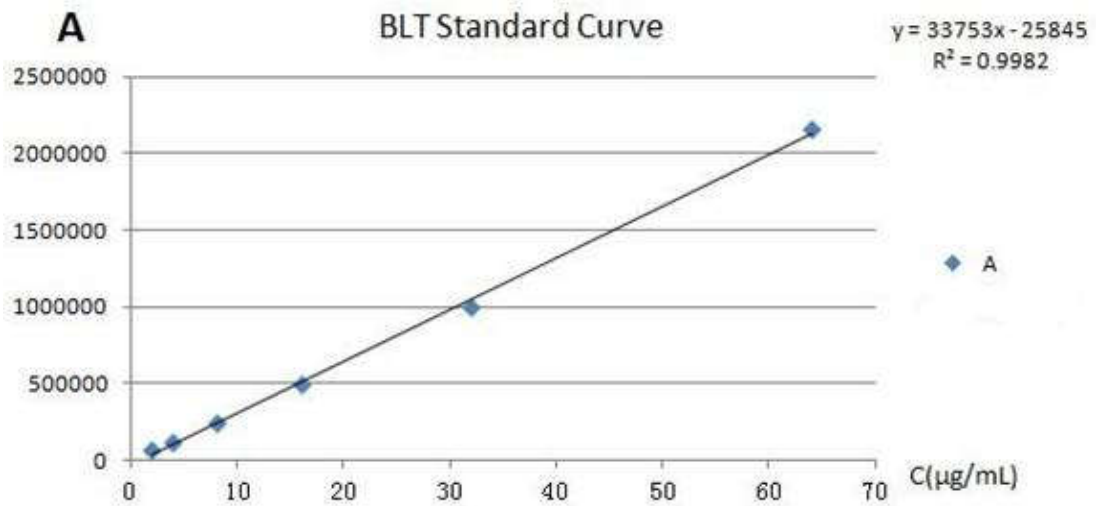


Fig. S18. Standard curve of BLT

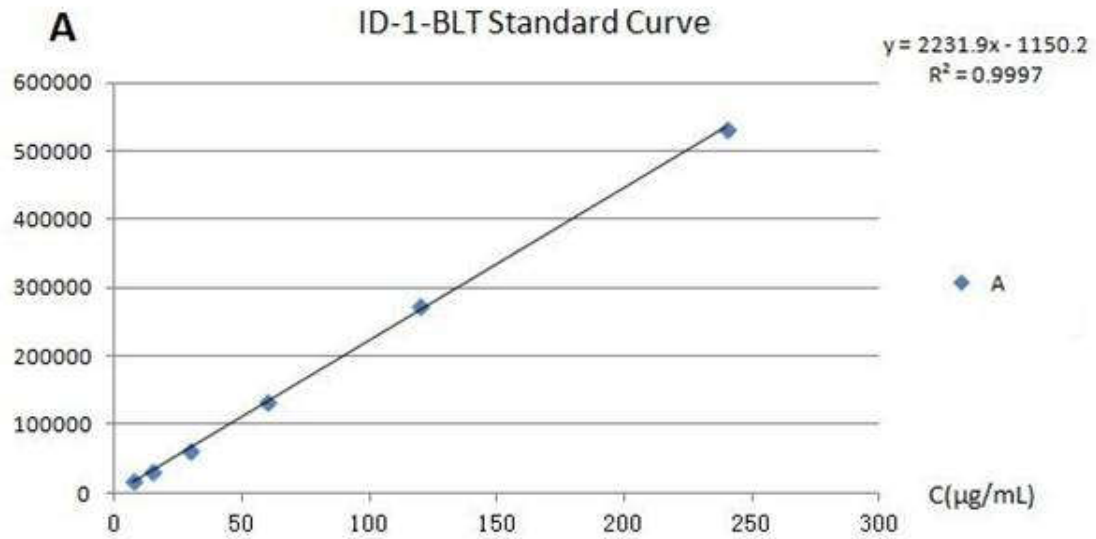


Fig. S19. Standard curve of **ID-1-BLT**

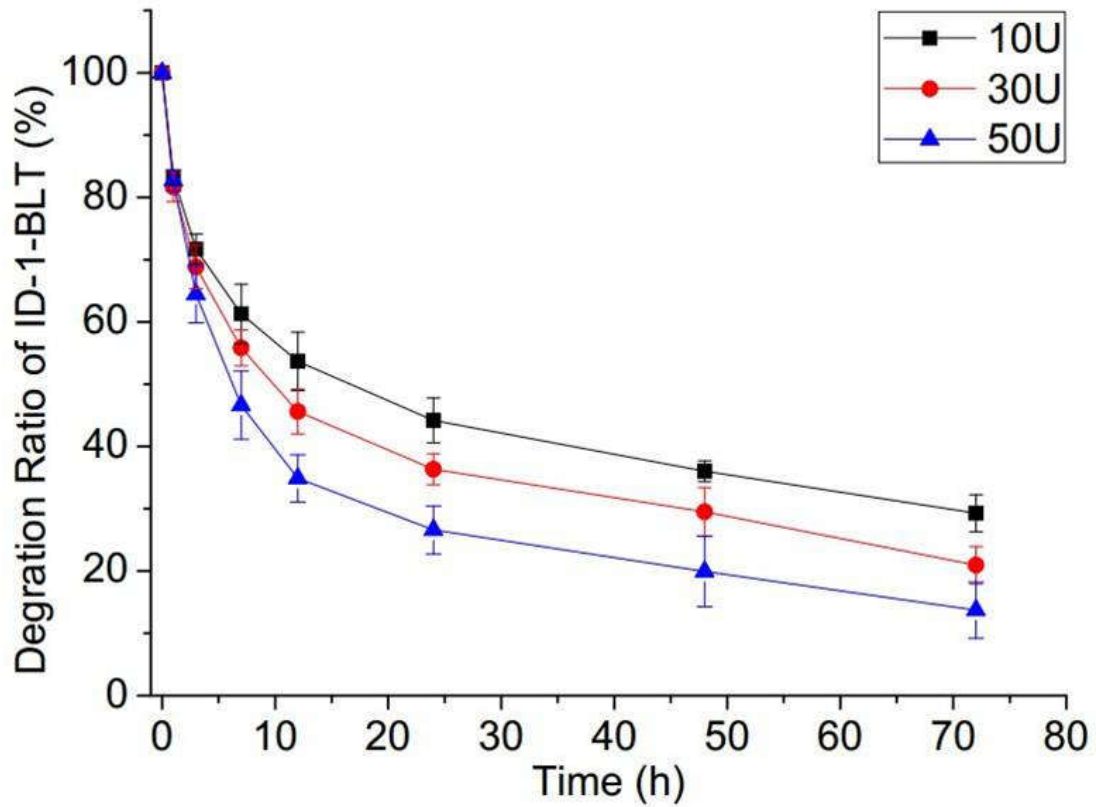


Fig. S20. Degradation ratio of **ID-1-BLT** incubated with different CES activity for 72h

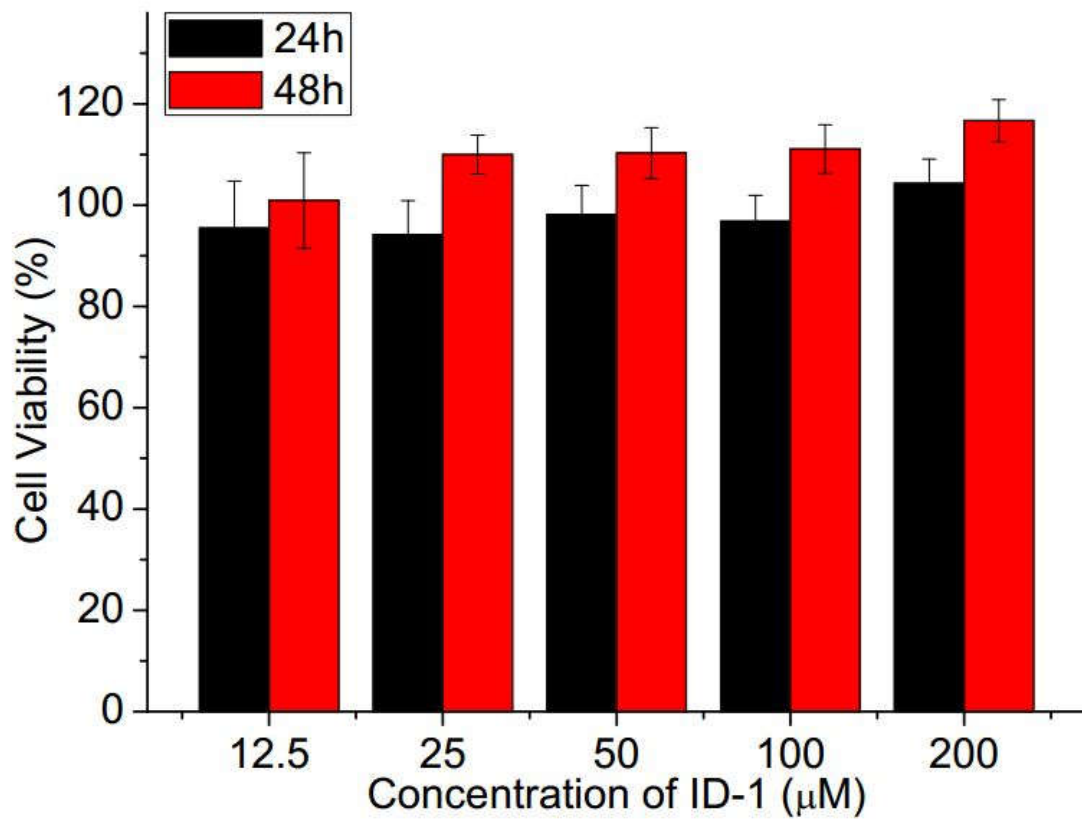


Fig. S21. Cell viability of DU145 cells after 24 h and 48 h of **ID-1**. Mean \pm SD (n=5).

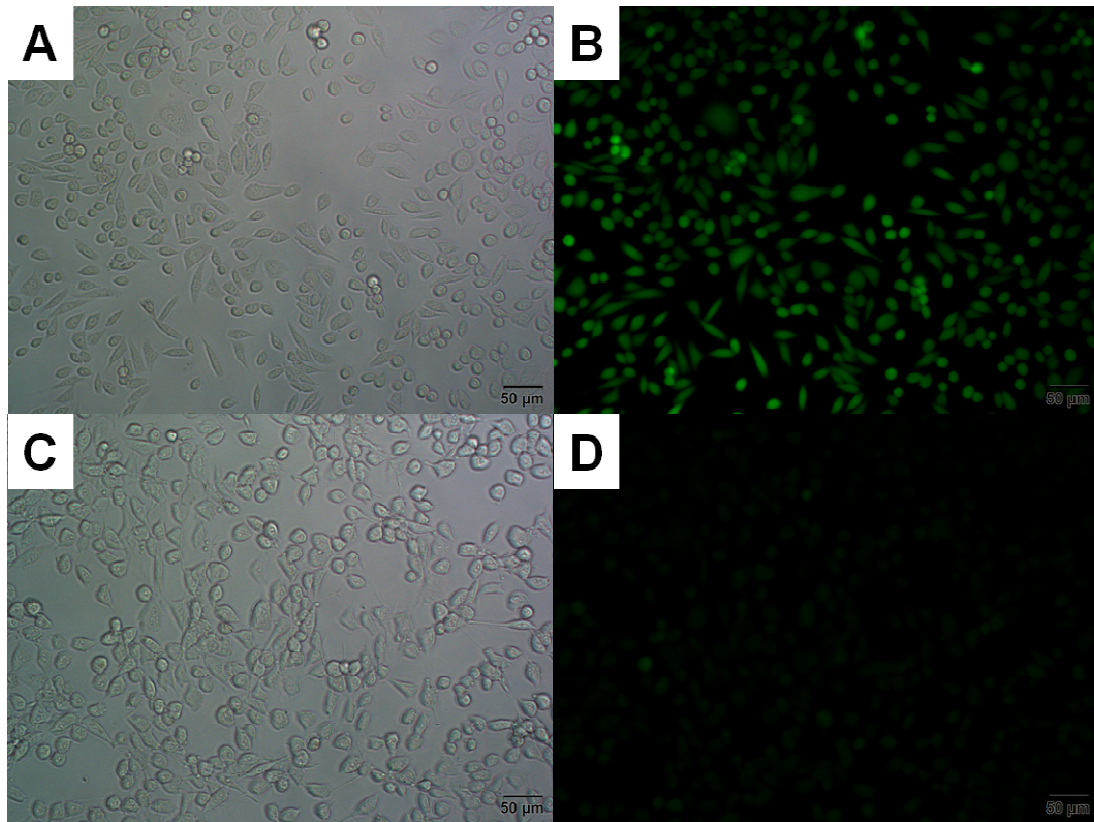


Fig. S22. CES activity assay of DU145 and NIH3T3 cells with Calcein-AM. (A) bright field and (B) fluorescence images of DU145 cells after Calcein-AM staining for 1 h; (C) bright field and (D) fluorescence images of NIH3T3 cells after Calcein-AM staining for 1 h.

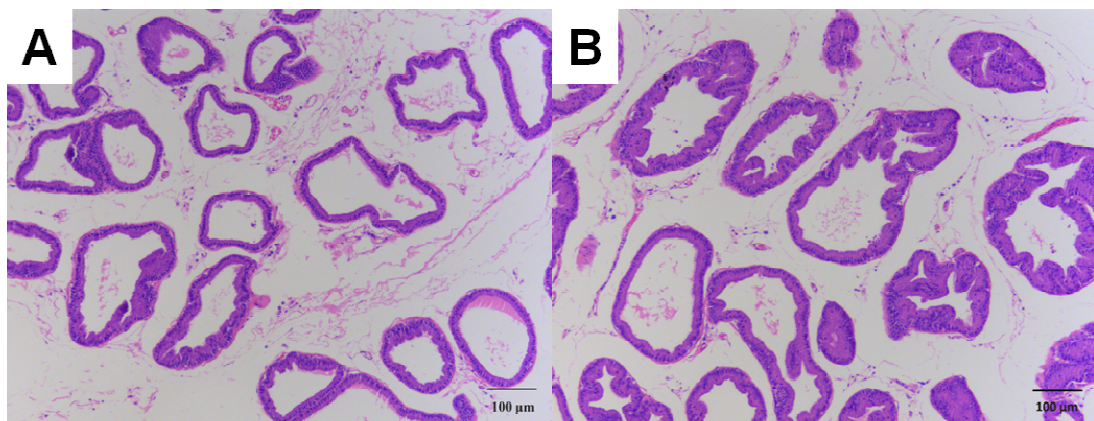


Fig. S23. H&E staining of the prostate tissue after intra-gland injections of (A) **ID-1** peptide and (B) saline in rats for 7 days

Table. S1. The parameters fitted with Ritger-Peppas models for 72 h drug release of **ID-1-BLT** in release buffers of varying pH

	k	R²	n
pH 5.5	0.0717	0.9407	0.4804
pH 6.5	0.0548	0.9072	0.4692
pH 7.4	0.0223	0.9506	0.5608

Table. S2. The parameters fitted with Ritger-Peppas models for 72 h drug release of **ID-1-BLT** in release buffers with varying units of CES

	k	R²	n
CES 50U/mL	0.0793	0.9692	0.5205
CES 10U/mL	0.0472	0.9630	0.5032
PBS	0.0216	0.9402	0.5555